

# Positive co-operative binding at two weak lysine-binding sites governs the Glu-plasminogen conformational change

Ulla CHRISTENSEN and Lone MØLGAARD

Department of Chemistry, Chemical Laboratory IV, University of Copenhagen, DK-2100 Copenhagen, Denmark

The kinetics of a series of Glu-plasminogen ligand-binding processes were investigated at pH 7.8 and 25 °C (in 0.1 M-NaCl). The ligands include compounds analogous to C-terminal lysine residues and to normal lysine residues. Changes of the Glu-plasminogen protein fluorescence were measured in a stopped-flow instrument as a function of time after rapid mixing of Glu-plasminogen and ligand at various concentrations. Large positive fluorescence changes (~10%) accompany the ligand-induced conformational changes of Glu-plasminogen resulting from binding at weak lysine-binding sites. Detailed studies of the concentration-dependencies of the equilibrium signals and the rate constants of the process induced by various ligands showed the conformational change to involve two sites in a concerted positive co-operative process with three steps: (i) binding of a ligand at a very weak lysine-binding site that preferentially, but not exclusively, binds C-terminal-type lysine ligands, (ii) the rate-determining actual-conformational-change step and (iii) binding of one more lysine ligand at a second weak lysine-binding site that then binds the ligand more tightly. Further, totally independent initial small negative fluorescence changes (~2–4%) corresponding to binding at the strong lysine-binding site of kringle 1 [Sottrup-Jensen, Claeys, Zajdel, Petersen & Magnusson (1978) *Prog. Chem. Fibrinolysis Thrombolysis* 3, 191–209] were observed for the C-terminal-type ligands. The finding that the conformational change in Glu-plasminogen involves two weak lysine-binding sites indicates that the effect cannot be assigned to any single kringle and that the problem of whether kringle 4 or kringle 5 is responsible for the process resolves itself. Probably kringle 4 and 5 are both participating. The involvement of two lysine binding-sites further makes the high specificity of Glu-plasminogen effectors more conceivable.

## INTRODUCTION

Native human Glu-plasminogen is the precursor of the fibrinolytic enzyme plasmin (EC 3.4.21.7). Glu-plasminogen contains five homologous triple-loop kringle domains (K1–K5), some of which possess lysine-binding sites (LBS) [1]. LBSs have specifically been identified and characterized in K1, K4 and K5 [2–10]. On the basis of their affinities to the classical antifibrinolytic amino acids, two to three classes of LBSs have been defined [11–14]. High-affinity or strong LBS are found in isolated K1 and K4 [4,6,9,10], but that of K4 apparently is hidden in intact Glu-plasminogen [5]. The LBS of K5 is a low-affinity or weak LBS, which is called the 'AH-site', since it binds the aminohexyl function of lysine and does not require a free carboxylate function [7,14].

Interactions at the LBSs are generally accepted to be important in the regulation of the fibrinolytic system [13,14], particularly the gross conformational change in Glu-plasminogen mediated by ligand binding to weak LBS, where apparently the AH-site [12,14–19] plays an important role. Fibrin and other effectors of Glu-plasminogen activation presumably exert their effects by inducing a change in the conformation and thereby making Glu-plasminogen more susceptible to the plasminogen-activating enzymes urokinase and tissue plasminogen activator [20–26]. Apparently, the role of the strong LBS of K1 is primarily to mediate interactions with  $\alpha_2$ -antiplasmin [14,27].

In order to elucidate these important physiological processes further we undertook stopped-flow fluorescence kinetic studies of the Glu-plasminogen ligand-binding processes. We have investigated a series of LBS ligands and here report that the ligand-induced Glu-plasminogen conformational change

involves binding at two weak LBSs. The reaction is an allosteric positive co-operative process that follows a classical regulatory mechanism. The results resolve the conflicting views as to whether K4 [5] or K5 [7,14,19] is responsible. It is our conclusion that, since two weak LBSs are involved, those of K4 and K5 are probably both participating.

## MATERIALS AND METHODS

### Reagents

Lysine-Sepharose 4B and aminohexyl (AH)-Sepharose 4B was obtained from Pharmacia (Uppsala, Sweden), 6-aminohexanoic acid (6-AHA) from Fluka (Buchs, Switzerland), and  $\alpha$ -N-acetyl-L-lysine methyl ester (Ac-Lys-OMe),  $\alpha$ -N-acetyl-L-lysine (Ac-Lys),  $\alpha$ -N-acetyl-L-lysine methyl ester (Ac-Lys-NH<sub>2</sub>) and  $\alpha$ -N-acetyl-L-lysine (Ac-Lys) were from Bachem (Bubendorf, Switzerland). *trans*-4-Aminomethylcyclohexanecarboxylic acid (t-AMCHA) was kindly provided as a gift from Kabi (Stockholm, Sweden), and Aprotinin (Trasylol) was from Bayer (Leverkusen, Germany). All other chemicals were analytical grade either from Fluka (Buchs, Switzerland) or Merck (Darmstadt, Germany).

Human Glu-plasminogen was prepared essentially as described in [28] from frozen human plasma kindly provided as a gift from Novo Nordisk A/S (Copenhagen, Denmark). It was separated from minor amounts of partially degraded plasminogen on AH-Sepharose 4B as in [29]. Glu-plasminogen was stored in 0.05 M-Tris/HCl/0.10 M-NaCl, pH 7.8, at –20 °C. The concentration of Glu-plasminogen was determined from absorbance measurements by using an  $A_{280}^{1\%}$  value of 16.2 [30].

Abbreviations used: LBS, lysine-binding site; K1–K5, kringle domains of Glu-plasminogen as defined in [1]; t-AMCHA, *trans*-4-aminomethylcyclohexanecarboxylic acid; 6-AHA, 6-aminohexanoic acid; Ac-Lys-OMe,  $\alpha$ -N-acetyl-L-lysine methyl ester; Ac-Lys,  $\alpha$ -N-acetyl-L-lysine; Ac-Lys-NH<sub>2</sub>,  $\alpha$ -N-acetyl-L-lysine; AH, aminohexyl.

### Stopped-flow kinetic experiments

Kinetic experiments were performed in a Hi-Tech Scientific PQ/SF-53 spectrofluorimeter equipped with a high-intensity xenon arc lamp and a fluorescence-enhancement device. The excitation wavelength was 280 nm, and the slit width was 5 mm. Light emitted from the reaction mixtures passed through a WG 320 filter before reaching the photomultiplier. A series of stopped-flow experiments were performed at 25 °C in 50 mM-Tris/HCl/0.1 M-NaCl, pH 7.8. After mixing the Glu-plasminogen (1.5  $\mu$ M final concn.) and the ligand the intrinsic protein fluorescence intensity (arbitrary units, V) was recorded for 200 ms.

Final concentrations of the ligand were: t-AMCHA (0, 0.5, 1, 5, 10, 50, 100, 375, 500 and 750  $\mu$ M, and 1, 1.25, 1.5, 2.5, 5, 12.5, 25, 50 and 100  $\mu$ M); 6-AHA (0, 20, 50, 100, 300 and 500  $\mu$ M, and 1.5, 3, 5, 10, 12.5, 20, 30, 50, 75, 100 and 200 nM); Ac-Lys (0, 13, 26, 52, 103, 258 and 517  $\mu$ M, and 1, 2, 4, 8, 20, 40, 60 and 80 mM); Ac-Lys-OMe (0, 25, 50, 100, 250, 400 and 500  $\mu$ M, and 1, 2, 4, 15, 30, 40, 50, 60 and 80 mM); Ac-Lys-NH<sub>2</sub> (0, 1, 10, 25 and 50 mM). Mixing was achieved in less than 1 ms. In each experiment 400 pairs of data were recorded, and sets of data from five or six experiments under identical conditions were averaged. Each averaged set of stopped-flow data were then fitted to a number of non-linear analytical equations using the Hi-Tech HS-1 Data Pro software. The regression analysis used was based on the Gauss-Newton procedure.

## RESULTS

### Conformational change of Glu-plasminogen

Fig. 1 shows the time course of a typical stopped-flow experiment measuring the large positive intrinsic protein fluorescence change obtained after mixing of Glu-plasminogen and t-AMCHA at concentrations known to induce a conformational change in Glu-plasminogen [15–18]. The fitted curve illustrated is the one corresponding to a single exponential progress (eqn. 1):

$$\Delta F([L], t) = \Delta F([L], \infty) [1 - \exp(-k_{\text{obs.}} t)] \quad (1)$$

where  $k_{\text{obs.}}$  is the observed first-order rate constant and  $\Delta F([L], t)$  is the relative fluorescence change observed at the actual ligand concentration,  $[L]$ , and time,  $t$ , which attains the value  $\Delta F([L], \infty)$  at equilibrium (8–10%). Eqn. (1) showed the most accurate fit to the measured data at all concentrations of all ligands employed.

The values of  $\Delta F([L], \infty)$  and  $k_{\text{obs.}}$  for the interactions of Glu-plasminogen with the ligands were obtained from fits to eqn. (1) at a number of concentrations of the ligands.

### t-AMCHA

The equilibrium values of the large positive change of the protein fluorescence [ $\Delta F([L], \infty)$ ] obtained after interaction of Glu-plasminogen with t-AMCHA are plotted against the concentration of t-AMCHA,  $[L]$ , in Fig. 2. Saturation of the signal, which is obtained at concentrations of t-AMCHA  $\geq 10$  mM, gives rise to a 10% change of the Glu-plasminogen fluorescence. Insert (i) of Fig. 2 shows a scale-up of the first part of the saturation curve. Its sigmoidal nature is clearly indicated. Insert (ii) of Fig. 2 shows a Hill plot of the same data. The slope of the line drawn has a value of 2.0. We thus observe a Hill coefficient of more than 1, which means that the large change in the protein fluorescence, corresponding to the Glu-plasminogen conformational change is part of a positive co-operative binding

process involving binding at (at least) two sites. The most plausible reaction model of the process is shown in Scheme 1. Binding of one ligand with dissociation constant,  $K_{\alpha}$  (step i), triggers a conformational change (step ii), that opens for the tighter binding of a second ligand with dissociation constant  $K_{\beta}$  ( $K_{\alpha} > K_{\beta}$ ) (step iii). Scheme 1 also shows the expressions of the ligand-concentration-dependencies of  $\Delta F([L], \infty)$  (eqn. 2) and of  $k_{\text{obs.}}$  (eqn. 3) which correspond with this reaction model (see the Appendix for derivation of the equations). Fig. 3 shows the result of fitting the expression to the  $k_{\text{obs.}}$  data. It is noteworthy that  $k_{\text{obs.}}$  goes through a minimum and saturates, as predicted by the model in Scheme 1. This is perhaps best seen from the inset to Fig. 3, which is a scale-up of the first part of the curve. The reaction model of Scheme 1 thus nicely accounts for the result of the Hill analysis and of the  $k_{\text{obs.}}$  data, whereas more simple models involving only one ligand, and also three-step models with other sequences of events, are inconsistent with the data (see the Appendix). The values obtained of the kinetic parameters of the t-AMCHA–Glu-plasminogen interaction are given in Table 1.

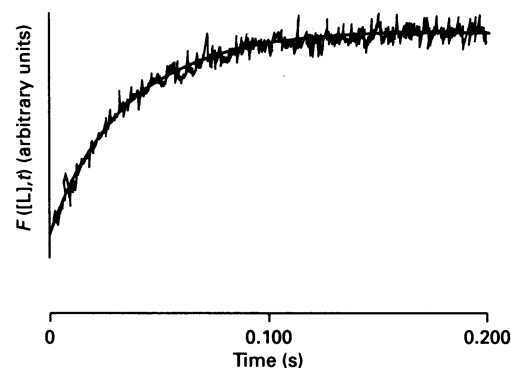


Fig. 1. Typical time course of the fluorescence signal obtained after mixing of Glu-plasminogen and ligand in the stopped-flow fluorimeter

In this example the final concentrations were: Glu-plasminogen, 1.5  $\mu$ M; t-AMCHA, 5 mM. The fitted curve corresponds to an overall first-order process (eqn. 1 in the text).

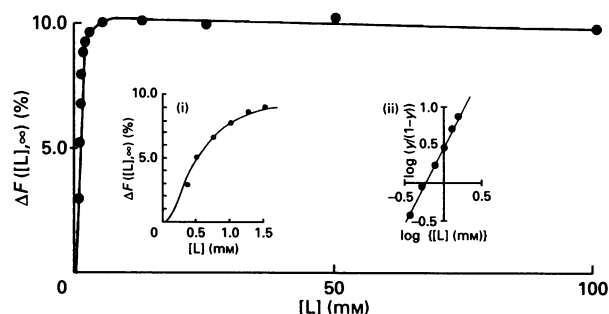
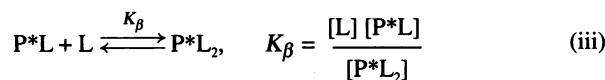
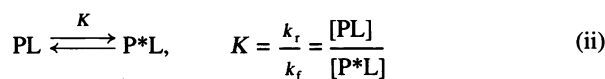
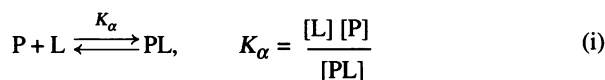


Fig. 2. Equilibrium values of the large positive change in the protein fluorescence [ $\Delta F([L], \infty)$ , % (eqn. 1)] obtained after interaction of Glu-plasminogen with t-AMCHA plotted against the concentration of t-AMCHA,  $[L]$ , in mM

Saturation of the signal, which is obtained at concentrations of t-AMCHA  $\geq 10$  mM, gives rise to a 10% change in the total Glu-plasminogen fluorescence. Experimental errors are within the size of the symbols. Inset (i) shows a scale-up of the first part of the saturation curve for  $[L] \leq 1.5$  mM. The line shown is that given by the fitted expression (eqn. 2 of Scheme 1). Inset (ii) shows the corresponding Hill plot;  $y$  is fractional saturation (see Fig. 6).



$$\Delta F([L], \infty) = \frac{\Delta F_{\max}([L], \infty)}{1 + \frac{KK_\beta}{[L](1 + K_\beta/[L])} + \frac{K_\alpha KK_\beta}{[L]^2(1 + K_\beta/[L])}} \quad (2)$$

$$k_{\text{obs.}} = \frac{k_f}{1 + K_\alpha/[L]} + \frac{k_r}{1 + [L]/K_\beta} \quad (3)$$

$$K_D = (K_\alpha K K_\beta)^{\frac{1}{2}} \quad (4)$$

**Scheme 1. Reaction scheme for ligand-induced Glu-plasminogen conformational change**

The model shown best explains the results for the relative fluorescence changes in the reactions of Glu-plasminogen, P, with ligands, L. The model relates the fluorescence change to the change of the Glu-plasminogen conformation and assumes a concerted reaction with three steps: (i) the formation of a first complex, PL, (ii) a change of the conformation of PL to another form, P\*L, and (iii) a second complexation resulting in a 1:2-Glu-plasminogen-ligand complex, P\*L<sub>2</sub>. The two ligands both interact with weak LBSs. The concentration-dependencies of experimentally determined parameters,  $\Delta F([L], \infty)$  and  $k_{\text{obs.}}$ , that correspond to this reaction scheme are given in eqns. (2) and (3) respectively. These parameters are defined in the text (eqn. 1).  $K_D$  is the overall dissociation constant,  $K_\alpha$  is that of the association complex, PL,  $K_\beta$  is that of the complex, P\*L<sub>2</sub>, for the dissociation of one ligand, and  $K$  is the equilibrium constant of step (ii).  $\Delta F_{\max}([L], \infty)$  is the maximal relative fluorescence change at saturating concentration of L.

**6-AHA**

As is illustrated in Figs. 4 and 5, results similar to those obtained for t-AMCHA were obtained with 6-AHA as the ligand inducing the conformational change of Glu-plasminogen. The values of its kinetic parameters obtained from fits to the expressions in Scheme 1 are also given in Table 1.

**Ac-Lys, Ac-Lys-OMe and Ac-Lys-NH<sub>2</sub>**

It is well known that the classical LBS ligands, t-AMCHA and 6-AHA, are able to induce a conformational change in Glu-plasminogen, but it is not known whether or not other ligands, such as Ac-Lys, Ac-Lys-OMe and Ac-Lys-NH<sub>2</sub>, which are expected to bind to the weak LBS of Glu-plasminogen, also induce the conformational change. Our results show that they do. Fig. 6(a) shows the Hill analyses of the  $\Delta F([L], \infty)$  data of Glu-plasminogen with each of the three ligands, and Fig. 6(b)

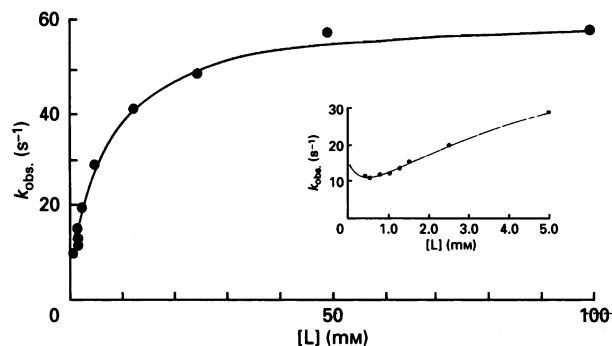


**Fig. 3. Glu-plasminogen-t-AMCHA interaction**

The observed value of the rate constant,  $k_{\text{obs.}}$ , was plotted against the concentration of t-AMCHA, [L], in mM. The inset shows a scale-up of the first part of the curve ( $[L] \leq 5$  mM). The experimental errors are within the size of the symbols. The line shown is obtained from fitting eqn. (3) (Scheme 1) to the data. The resulting parameters are given in Table 1.

**Table 1. Kinetic parameters of the ligand-induced Glu-plasminogen conformational-change process**

$K_D$  is the overall dissociation constants for the concerted process (eqn. 4, Scheme 1).  $K_\alpha$  and  $K_\beta$  are the individual dissociation constants of the Glu-plasminogen-ligand complexes, PL and P\*L<sub>2</sub> respectively (i and iii, Scheme 1).  $K$  is the equilibrium constant of the conformational-change step (ii, Scheme 1). The corresponding first-order rate constants for the forward and reversed reaction are  $k_f$  and  $k_r$  respectively. The parameters given are obtained by computer fits of eqns. (2) and (3) (Scheme 1) to the experimental data using the non-linear least-squares program GRAFIT (Erithacus Software). (Figs. 2, 3, 5, 6a and 6b). The standard errors of the estimates are, for values marked '~', approx. 30%; otherwise the error is 10%.

Ligand	$K_D$ (mM)	$K_\alpha$ (mM)	$K$	$K_\beta$ (mM)	$k_f$ (s <sup>-1</sup> )	$k_r$ (s <sup>-1</sup> )
t-AMCHA	0.8	6.4	0.2	0.4	62	15
6-AHA	2.7	36	0.2	1.1	71	14
Ac-Lys	11	~ 120†	0.2*	~ 5	~ 100†	~ 20
Ac-Lys-OMe	56	~ 400†	0.2*	~ 40	~ 225†	~ 45
Ac-Lys-NH <sub>2</sub>	76	~ 1400†	0.2*	~ 20	~ 150†	~ 30

\* Assumed values, not experimentally determinable.

† These values apply only if the assumption that the  $K$  value of all the ligands is the same is valid.

shows the  $k_{\text{obs.}}$  curves. Saturation was not obtained at soluble concentrations of the ligands, but the minima are obvious. The reaction model of Scheme 1 is not necessarily correct for these ligands, but it certainly can account for the observed results. Only the overall dissociation constant,  $K_D [= (K_\alpha K K_\beta)^{\frac{1}{2}}]$ , estimates of  $K_\beta$  and the rate constant,  $k_r$ , can be determined from the data. It is further apparent that  $K_\alpha$  values all are greater than 80 mM (Table 1).

**Kringle-1 binding**

The value of the fluorescence of Glu-plasminogen in the absence of ligands did not coincide with that at zero time (that is, approx. 1 ms) in the presence of ligands, except for Ac-Lys-OMe. Within the dead time of the instrument, a small negative change of the fluorescence (2-4%; saturating level) occurred. This was found to be ligand-concentration-dependent, corresponding to binding of ligands at the strong LBS. The results are

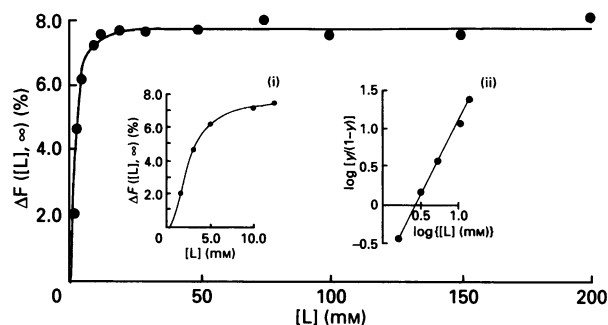


Fig. 4. Glu-plasminogen–6-AHA interaction,  $\Delta F([L], \infty)$

Shown is a plot of  $\Delta F([L], \infty)$  versus the concentration of 6-AHA. The experimental errors are included in the size of the symbols. Inset (i) shows a scale-up of the first part of the curve. The line is that obtained from fitting eqn. (2) (Scheme 1) to the data. Inset (ii) shows the corresponding Hill plot.

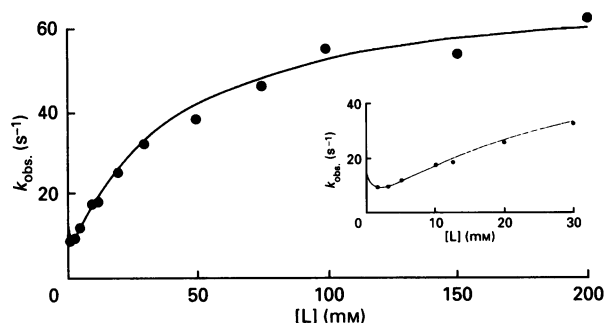


Fig. 5.  $k_{\text{obs}}$  of the Glu-plasminogen–6-AHA interaction

The observed value of the rate constant,  $k_{\text{obs}}$ , is plotted against the concentration of 6-AHA,  $[L]$ , in mM. The experimental errors are within the size of the symbols. The inset shows a scale-up of the first part of the curve ( $[L] \leq 12$  mM). The line shown is obtained from fitting eqn. (3) (Scheme 1) to the data. The resulting parameters are given in Table 1.

illustrated in Fig. 7 and the dissociation constants obtained for the strong LBS interactions are given in Table 2.

## DISCUSSION

In the present work the kinetics of the formation of complexes of Glu-plasminogen with LBS ligands were studied using measurements of changes of the intrinsic protein fluorescence of Glu-plasminogen after rapid mixing in a stopped-flow instrument. Particular attention was paid to the ligand-induced conformational change of Glu-plasminogen known to occur when certain ligands bind to its weak LBSs [12,15–19], one of which is the AH-site of the miniplasminogen part of the molecule [14]. The compounds studied were: t-AMCHA, 6-AHA, Ac-Lys, Ac-LysO-Me and Ac-Lys-NH<sub>2</sub>. This series was chosen with the aim of comparing the mechanisms of reactions and the reactivities of ligands analogous to C-terminal lysine residues with those of ligands analogous to normal lysine residues of proteins. Both types of ligands apparently are important in fibrinolysis [7,14,31].

### Reaction mechanism of the conformational change

Detailed studies of the ligand-induced conformational change of Glu-plasminogen were performed. The results show that the

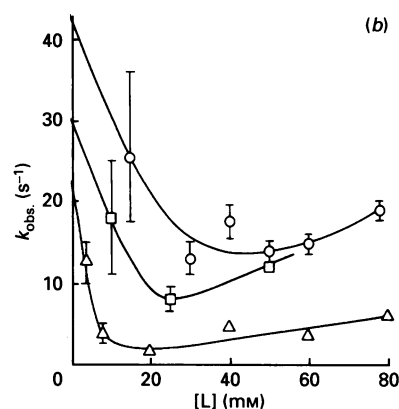
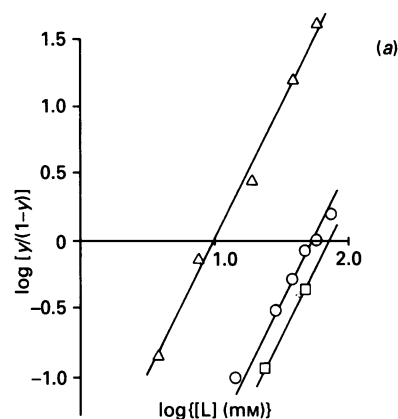


Fig. 6. Glu-plasminogen interactions with Ac-Lys, Ac-Lys-NH<sub>2</sub> and Ac-Lys-OMe

(a) Hill plots using the equilibrium values of the relative fluorescence changes obtained at various concentrations,  $[L]$ , of Ac-Lys ( $\Delta$ ), Ac-LysOMe ( $\circ$ ) and Ac-LysNH<sub>2</sub> ( $\square$ ).  $y$  is the fractional saturation  $[\Delta F([L], \infty) / \Delta F_{\text{max}}([L], \infty)]$  (eqn. 2, Scheme 1). (b) Observed values of the rate constant,  $k_{\text{obs}}$ , plotted against the concentrations,  $[L]$ , of Ac-Lys ( $\Delta$ ), Ac-LysOMe ( $\circ$ ) and Ac-LysNH<sub>2</sub> ( $\square$ ). The lines correspond with eqn. (3) (Scheme 1) with the parameter values given in Table 1.

process is a concerted reaction that, in addition to the actual conformational change, involves binding of the ligand not at one, but at two, weak LBSs of Glu-plasminogen (Table 1). This is an interesting new finding, namely that the conformational change of Glu-plasminogen involves binding of ligands at two weak sites in a positive co-operative process (Figs. 2, 4 and 6). It is noteworthy, furthermore, that all of the ligands studied are able to provoke the change and that the reaction mechanism (Scheme 1) apparently (Figs. 3, 5 and 6) is the same for all the ligands: (i) binding at one particular very weak LBS triggering (ii) the change of the Glu-plasminogen conformation, resulting in the opening of another weak LBS, which (iii) binds a ligand more tightly than the first one (Scheme 1 and Table 1). This is a co-operative mechanism, and the physiological importance of such mechanisms is to obtain regulation of a process within a narrow range of concentrations of the ligand involved, e.g. as in the classical oxygen–haemoglobin binding curve. A simple binding curve changes the degree of saturation over a far greater range of concentrations. The conformational change of Glu-plasminogen, which is important for its rate of activation into plasmin [22–26], then can be turned on and off with small changes of the concentration of the appropriate ligand.

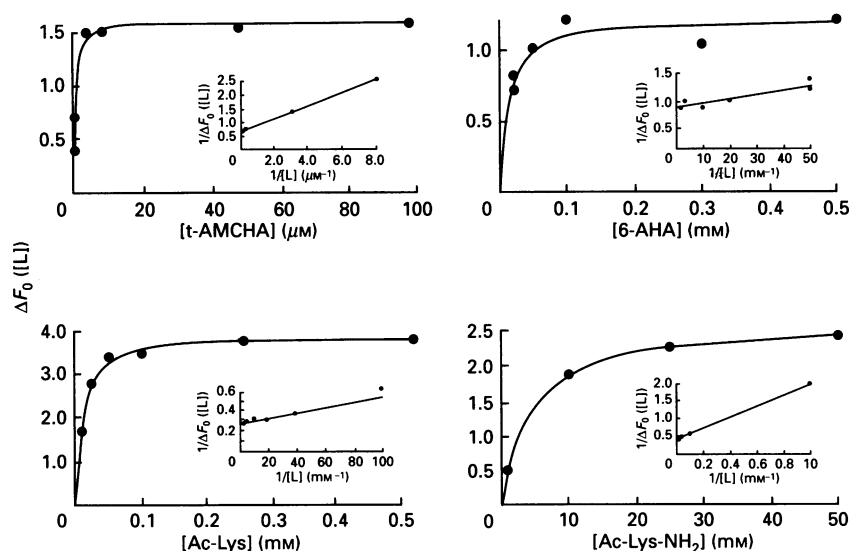


Fig. 7. Small, negative fluorescence changes observed at low concentrations of the ligands corresponding with binding at the strong LBS of K1 of Glu-plasminogen

The zero-time ( $< 1$  ms) negative  $\Delta F_0(\text{LL})$  is plotted against the concentration of the ligand in question. Ac-Lys-OMe gave a  $\Delta F_0(\text{LL})$  of 0. The insets illustrate the double-reciprocal plots of the data. Experimental errors were 3–7%.

Table 2. Dissociation constants,  $K_0$ , of ligands complexing the strong LBS of K1 of Glu-plasminogen

Ligand	$K_0$ ( $\mu\text{M}$ )		
	Glu-plasminogen (The present work)*	Glu-plasminogen (Litt.)†	K1 or K1–K2–K3 fragments (Litt.)†
t-AMCHA	0.4	1.1 [8]	1.2 [3]
6-AHA	11	9 [12]	2.9–3.2 [35]
Ac-Lys	10		17 [4]
Ac-Lys-NH <sub>2</sub>	4400		
Ac-Lys-OMe	$\infty$		

\* Values obtained from the experiments illustrated in Fig. 7.

† (Litt.), literature values.

### Ligand specificity

The ligands studied here show no differences in their mechanisms of inducing Glu-plasminogen conformational changes. Both types, namely those analogous to C-terminal lysine residues and those analogous to normal lysine residue in proteins, induce the effect, but their reactivities differ. The values of the overall equilibrium constants,  $K_D = (K_a K_b)^{1/2}$ ; Table 1, evidently show specificity in the order:

t-AMCHA > 6-AHA > Ac-Lys > Ac-Lys-OMe > Ac-Lys-NH<sub>2</sub>

Thus some more general principles emerge regarding the features that are important for ligand-induced Glu-plasminogen conformational change. To bind each of the two weak LBSs it seems ideal if the ligand contains a formed structural unit with two lysine residues suitably placed to be held in the proper orientation to the Glu-plasminogen-binding sites. The reaction with such a performed 'dimer' should be favoured over that with two 'monomers'. Further, it seems advantageous if at least one of the lysine residues is C-terminal. This explains some of the known features of Glu-plasminogen interactions. Fibrin, fibrin fragments, particularly partially plasmin-cleaved fragments with

C-terminal lysine residues, and polylysines, are known to interact with Glu-plasminogen and effect its rate of activation [10,13,21,25,26,31–33]. Such effects are not exerted by proteins in general, although most proteins contain several externally placed lysine side chains. It seems highly likely that polylysine can provide a pair of suitably placed lysine residues, one of which is a C-terminal lysine residue, whereas proteins in general cannot. The specific interactions of fibrin and fibrin fragments with Glu-plasminogen probably also reflect the presence of certain lysine pairs placed in proper orientation in these molecules. The interaction of Glu-plasminogen with AH-Sepharose is another example.

### Other LBSs

The results discussed above show that ligand-induced conformational changes of Glu-plasminogen involves two weak LBSs. Independent binding at a strong LBS, giving rise to small, but significant, negative changes of the fluorescence, was also observed for all of the ligands, except for Ac-Lys-OMe (Fig. 7). The dissociation constants ( $K_0$  values) obtained for t-AMCHA and 6-AHA correlate well with those reported previously of the Glu-plasminogen LBS, which has been assigned to K1 [4–6,9,12,18]. Binding at this site was achieved within the dead time of the stopped-flow instrument ( $< 1$  ms) and is apparently a simple fast 1:1 complexation. The small fluorescence signal is probably due to perturbations of Trp-62 and/or Tyr-72 of K1 [35]; no change of the Glu-plasminogen conformation occurs at these low concentrations of the ligands.

Our results indicate that the strong LBS is indeed specifically interacting with C-terminal lysine residues, as suggested previously [14,32], since there is a total lack of reaction with Ac-Lys-OMe. On the other hand, interaction with Ac-Lys-NH<sub>2</sub> does occur, but the binding of this compound is very weak.

### Role of LBSs

As suggested previously, the weak LBSs of Glu-plasminogen probably are very important to consider if we want to understand the regulation of fibrinolysis [14]. The finding that two such sites are allosterically involved in the ligand-induced conformational change of Glu-plasminogen may resolve the apparently

conflicting previous results on which of the kringles participates: the LBS of K4 [5] or the AH-site of K5 [14]. The two weak LBSs of K4 and K5 are probably both involved. However, Glu-plasminogen also contains a strong LBS in K1, saturation of which abolishes binding of  $\alpha_2$ -antiplasmin [27] and of histidine-rich glycoprotein [34], but does not induce the conformational change that seems to be important in determining the rate of Glu-plasminogen activation [22–26]. Clearly the interplay between Glu-plasminogen and its ligands is not yet fully understood, but it is necessary to distinguish the effects of interaction at K1 from those of the weak LBSs.

This work was supported by grants from Grete and Hans Lundbeck's Legat (Foundation) (grant L. 24/90), from the Danish Science Research Council (grant 11-7542) and from the Carlsberg Foundation (grants 88-0093/40 and 89-0098/10).

## REFERENCES

- Sottrup-Jensen, L., Claeys, H., Zajdel, M., Petersen, T. E. & Magnusson, S. (1978) *Prog. Chem. Fibrinolysis Thrombolysis* **3**, 191–209
- Rickli, E. E. & Otavsky, W. I. (1975) *Eur. J. Biochem.* **59**, 441–447
- Markus, G., Camiolo, S. M., Sottrup-Jensen, L. & Magnusson, S. (1981) *Prog. Fibrinolysis* **5**, 125–128
- Lerch, P. G., Rickli, E. G., Lergier, W. & Gillissen, D. (1980) *Eur. J. Biochem.* **107**, 7–13
- Váli, Z. & Patthy, L. (1982) *J. Biol. Chem.* **257**, 2104–2110
- Llinás, M., DeMarco, A., Hochschwender, S. M. & Laursen, R. A. (1983) *Eur. J. Biochem.* **135**, 379–391
- Thewes, T., Constantine, K., Byeon, I. L. & Llinás, M. (1990) *J. Biol. Chem.* **265**, 3906–3915
- Trexler, M., Váli, Z. & Patthy, L. (1982) *J. Biol. Chem.* **257**, 7401–7406
- Motta, A., Laursen, R. A., Llinás, M., Tulinsky, A. & Park, C. H. (1987) *Biochemistry* **26**, 3827–3836
- Suenson, E., Lützen, O. & Thorsen, S. (1984) *Eur. J. Biochem.* **140**, 513–522
- Markus, G., Evers, J. L. & Hobika, G. H. (1978) *J. Biol. Chem.* **253**, 733–739
- Markus, G., De Pasquale, J. L. & Wissler, F. C. (1978) *J. Biol. Chem.* **253**, 727–732
- Wiman, B. & Collen, D. (1978) *Nature (London)* **272**, 549–550
- Christensen, U. (1984) *Biochem. J.* **223**, 413–421
- Violand, B. N., Byrne, R. & Castellino, F. J. (1978) *J. Biol. Chem.* **253**, 5395–5401
- Mangel, W. F., Lin, B. & Ramakrishnan, V. (1990) *Science* **248**, 69–73
- Alkjær sig, N. (1964) *Biochem. J.* **93**, 171–183
- Markus, G., Pirore, R. L. & Wissler, F. C. (1979) *J. Biol. Chem.* **254**, 1211–1216
- Christensen, U. & Mølgaard, L. (1991) *FEBS Lett.* **278**, 204–206
- Thorsen, S., Kok, P. & Astrup, T. (1974) *Thromb. Diath. Haemorrh.* **32**, 325–340
- Thorsen, S. (1975) *Biochim. Biophys. Acta* **393**, 55–65
- Christensen, U. (1977) *Biochim. Biophys. Acta* **481**, 638–647
- Hoylaerts, M., Rijken, D. C., Lijnen, H. R. & Collen, D. (1982) *J. Biol. Chem.* **257**, 2912–2919
- Peltz, S. W., Hardt, T. A. & Mangel, W. F. (1982) *Biochemistry* **21**, 2798–2804
- Rånby, M. (1982) *Biochim. Biophys. Acta* **704**, 461–469
- Petersen, L. C., Brender, J. & Suenson, E. (1985) *Biochem. J.* **225**, 144–158
- Wiman, B., Lijnen, H. R. & Collen, D. (1979) *Biochim. Biophys. Acta* **579**, 142–154
- Deutsch, D. G. & Mertz, E. T. (1970) *Science* **170**, 1095–1096
- Nieuwenhuizen, W. & Traas, D. W. (1989) *Thromb. Haemostasis* **61**, 208–210
- Christensen, U. (1988) *Biochim. Biophys. Acta* **957**, 258–265
- Rákóczi, I., Wiman, B. & Collen, D. (1978) *Biochim. Biophys. Acta* **540**, 295–300
- Christensen, U. (1985) *FEBS Lett.* **182**, 43–46
- Lucas, M. A., Fretto, L. J. & McKee, P. A. (1983) *J. Biol. Chem.* **258**, 4249–4256
- Lijnen, H. R., Hoylaerts, M. & Collen, D. (1980) *J. Biol. Chem.* **255**, 10214–10222
- Matsuka, Y. V., Novokhatny, V. V. & Kudinov, S. A. (1990) *Eur. J. Biochem.* **190**, 93–97
- Motta, A., Laursen, R. A., Llinás, M., Tulinsky, A. & Park, C. H. (1987) *Biochemistry* **26**, 3827–3836

## APPENDIX

The equations of Scheme 1 which correspond with the reaction model suggested for the plasminogen conformational-change process, are derived as follows (for convenience the numbering of equations follows on from that in the main paper).

$\Delta F([L], \infty)$ , the equilibrium value of the fluorescence change at ligand concentration  $[L]$ :

See eqn. (2), Scheme 1

The total concentration of the plasminogen (P) is equal to the sum of the various species present (eqn. 5):

$$[P_0] = [P] + [PL] + [P^*L] + [P^*L_2] \quad (5)$$

Step (ii) of Scheme 1 leads to a change in conformation, so that the sum of the two changed species,  $[P^*L]$  and  $[P^*L_2]$ , is responsible for the fluorescence change, that is:

$$\Delta F([L], \infty) = A([P^*L] + [P^*L_2]) \quad (6)$$

where  $A$  is some arbitrary factor. Similarly for the limit value at saturation with  $L$ ,

$$\Delta F_{\max.}([L], \infty) = A[P_0] \quad (7)$$

then:

$$\Delta F([L], \infty) = \frac{\Delta F_{\max.}([L], \infty)([P^*L] + [P^*L_2])}{[P_0]} \quad (8)$$

or, from eqn. (5):

$$\Delta F([L], \infty) = \frac{\Delta F_{\max.}([L], \infty)}{1 + \frac{[P] + [PL]}{[P^*L] + [P^*L_2]}} \quad (9)$$

the denominator of which may be rearranged to

$$1 + \frac{[P]}{[P^*L_2](1 + [P^*L]/[P^*L_2])} + \frac{[PL]}{[P^*L_2](1 + [P^*L]/[P^*L_2])} \quad (10)$$

From the definitions of the equilibrium constants of the steps (i), (ii) and (iii) of Scheme 1 the equilibrium ratios of the protein species are known and can be expressed in terms of  $K$  values and  $[L]$ ; the denominator then becomes that of eqn. (2) in Scheme 1.

### The observed rate constant, $k_{\text{obs}}$ (eqn. 3, Scheme 1)

The change of fluorescence observed as a function of time,  $t$ , is given by:

$$d([P^*L]_t + [P^*L_2]_t)/dt = k_r[PL]_t - k_r[P^*L]_t \quad (11)$$

In conditions of fast equilibrium in steps (i) and (iii) compared

with that of the conformational-change step (ii), eqns. (i) and (iii) are obeyed in the observed course of the reaction, so that, from eqn. (5):

$$[P_o] = [PL]_t(K_\alpha/[L] + 1) + [P^*L]_t(1 + [L]/K_\beta) \quad (12)$$

and

$$d([P^*L]_t + [P^*L_2]_t)/dt = (1 + [L]/K_\beta) d([P^*L]_t)/dt \quad (13)$$

Eqn. (11) may be transformed into a simple linear first-order differential equation in  $[P^*L]_t$ :

$$(1 + [L]/K_\beta) d([P^*L]_t)/dt = k_t \frac{[P_o]}{1 + K_\alpha/[L]} - \left( \frac{k_t(1 + [L]/K_\beta)}{1 + K_\alpha/[L]} + k_r \right) [P^*L]_t \quad (14)$$

or

$$d([P^*L]_t)/dt = \text{constant} - (k_{\text{obs.}}) [P^*L]_t \quad (15)$$

where  $k_{\text{obs.}}$  is that given in eqn. (3) of Scheme 1.

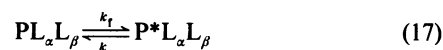
### Other reaction models

Two other mechanisms would give rise to a second-order dependence of the fluorescence signal change on the ligand concentrations: (a) one in which the conformational-change step follows after binding of two ligand molecules, and (b) one in which the conformational-change step is the first step and each of the two ligand molecules binds only the conformationally changed form of the plasminogen.

(a) For the first of these the Mass Conservation Law leads to:

$$\begin{aligned} P_o &= P + PL_\alpha + PL_\beta + PL_\alpha L_\beta + P^*L_\alpha L_\beta \\ &= PL_\alpha L_\beta \{ [L]^2 / K_\alpha K_\beta + [L] / K_\beta + [L] / K_\alpha + 1 \} + P^*L_\alpha L_\beta \quad (16) \\ &= f(L^2, L) PL_\alpha L_\beta + P^*L_\alpha L_\beta \end{aligned}$$

Where fast equilibration in the ligand-association steps is assumed. The conformational change step is:



and its rate:

$$\frac{d(P^*L_\alpha L_\beta)_t}{dt} = k_t(PL_\alpha L_\beta)_t - k_r(P^*L_\alpha L_\beta)_t \quad (18)$$

which, when  $PL_\alpha L_\beta$  is substituted using eqn. (16), becomes:

$$\frac{d(P^*L_\alpha L_\beta)_t}{dt} = \frac{k_t P_o}{f(L^2, L)} - \left( \frac{k_t}{f(L^2, L)} + k_r \right) (P^*L_\alpha L_\beta)_t \quad (19)$$

so that:

$$k_{\text{obs.}} = k_r + k_t / (1 + L/K_\alpha) (1 + L/K_\beta) \quad (20)$$

which is an ever-decreasing function of the ligand concentration.

(b) For the second of the mechanisms mentioned above:

$$\begin{aligned} P_o &= P + P^* + P^*L_\alpha + P^*L_\beta + P^*L_\alpha L_\beta \\ &= P + P^*(1 + L/K_\alpha + L/K_\beta + L^2/K_\alpha K_\beta) \end{aligned} \quad (21)$$

The conformational change step is:



which is initially in an equilibrium, but perturbed when ligand is added and  $P^*L$  complexes are formed. The rate of establishing the new equilibrium is given by:

$$-\frac{dP_t}{dt} = k_t P_t - k_r P^*_t \quad (23)$$

which, by analogy to the derivation under (a), leads to:

$$k_{\text{obs.}} = k_t + k_r / (1 + L/K_\alpha) (1 + L/K_\beta) \quad (24)$$

It is thus found that neither of the models, (a) or (b), are compatible with the results observed and presented in Figs. 3, 5 and 6.